

Trans. Nonferrous Met. Soc. China 22(2012) 1878-1883

Transactions of Nonferrous Metals Society of China

www.tnmsc.cn

# Evolution in microstructure and mechanical properties during back-annealing of AlMnFeSi alloy

WANG Ning<sup>1</sup>, Jarl Erik FLATØY<sup>1</sup>, LI Yan-jun<sup>2</sup>, Knut MARTHINSEN<sup>1</sup>

- Department of Materials Science and Engineering, Norwegian University of Science and Technology, NO-7491, Trondheim, Norway;
  - 2. SINTEF Materials and Chemistry, NO-7465, Trondheim, Norway

Received 10 November 2011; accepted 25 June 2012

**Abstract:** An Al–Mn–Fe–Si model alloy was subjected to two homogenization treatments, to achieve materials with different levels of Mn in solid solution and dispersoid densities, followed by cold rolling and back-annealing. Characterization of homogenization and deformation structures with respect to the effect of different microchemistries and strains on the structures was performed. Time–temperature–transformation (TTT) diagram with respect to precipitation and recrystallisation as a basis for analysis of the degree of concurrent precipitation was established. The TTT-diagram shows a strong effect of Mn concentration in solid solution and dispersoid density on the softening behavior. Recrystallization which finishes without the effect of concurrent precipitation results in an even, fine and equiaxed grain structure. Precipitation prior to or during recrystallization (concurrent) does retard the softening kinetics and leads to a coarse grain structure. However, the effect also depends on the duration of recrystallization and amount of precipitation. Recrystallization proceeding over a long time combined with a large amount of concurrent precipitation has a strong effect, otherwise the effect will be limited. Pre-existing fine and dense dispersoids (mean size 0.1 µm) before back-annealing do also lead to a coarse grain structure after recrystallization no matter whether additional concurrent precipitation occurs.

**Key words:** homogenization treatment; dispersoid phase; solid solution; back-annealing; recrystallization; concurrent precipitation; TTT-diagram

#### 1 Introduction

An increased use of recycled aluminium requires the development of new tailor made alloys and an optimisation of the thermo-mechanical processing routes to handle the corresponding changes and variations of compositions (alloying elements impurities). Typically, alloying elements like Mn, Fe and Si will accumulate in secondary alloys, which may strongly affect the microstructural evolution and associated mechanical properties during processing. It is well established that the dispersoids retard the recovery and recrystallization kinetics and have a large effect on the final grain size and texture of the alloys [1–11]. However, the effects and mechanisms behind are neither well understood nor quantitatively described. The objective of the present work was to investigate the effect of different microchemistries (solid solution levels, constituent particles and dispersoids) on the softening behavior of a cold rolled AlMnFeSi alloy.

The work is motivated by the need to improve existing physically based computer models to adequately describe the softening behaviour in recycle based aluminium alloys strongly influenced by dispersoids and concurrent precipitation.

### 2 Experimental

In the present work, the investigated material was a commercial DC-cast AA3xxx extrusion billet, supplied by Hydro Aluminium. The as-received material was in as-cast state with the chemical composition given in Table 1. Slabs were machined from the central region of the as-cast billet with three gauges of thickness. For each gauge of thickness, the slabs were homogenized with two different procedures to get different microchemistries in terms of the amount of Mn in solid solution (potential for subsequent precipitation) and different volume fractions and sizes of dispersoids. The two different material conditions were labeled as C2-1 and C2-2, as shown in Table 2. The homogenization treatments were performed

**Foundation item:** Project (KMB: 193179/I40) supported by the Research Council of Norway **Corresponding author:** WANG Ning; Tel: +47-48047203; E-mail: ning.wang@material.ntnu.no DOI: 10.1016/S1003-6326(11)61401-5

**Table 1** Chemical composition of AA3xxx alloy used in the present work (mass fraction, %)

Si	Fe	Mn	Cu	Others
0.152	0.530	0.970	0.001	< 0.001

**Table 2** Two homogenization procedures and different concentration levels of Mn in solid solution

Sample	$w(Mn_{ss})/\%$	Homogenization procedure
C2-1	0.35	50 °C/h up to 600 °C+24 h, 600 °C+quenching
C2-2	0.23	50 °C/h up to 450 °C+4 h, 450 °C + quenching

in an air circulation furnace with a temperature accuracy of  $\pm 2$  K, starting from room temperature (about 20 °C) with a heating rate of 50 K/h and subsequent heating procedures as described in Table 2. Materials were water quenched to room temperature at the end of the homogenization procedure. Electrical conductivity was measured by a Sigmascope EX 8 at room temperature of about 293 K (20 °C). Back scatter electron (BSE) images obtained in a scanning electron microscope (SEM) were used to characterize constituent particles and dispersoids. Characteristic size parameters of constituent particles, equivalent diameter d, Feret diameter, area fraction and number density were measured by the image analysis software IMAGE-PRO.

The homogenized materials were cold rolled to different strains ( $\varepsilon$ ) in the range of 0.7–3.0. The rolled sheets were subsequently isothermally back-annealed in a salt bath at different temperatures in the range of 300-500 °C and time in the range of 5-10<sup>5</sup> s, followed by water quenching to room temperature. The softening and precipitation behaviour during annealing was followed by Vickers hardness and electrical resistivity measurements performed on the RD-ND plane of sheets. Time-temperature-transformation (TTT) diagrams with respect to precipitation and recrystallisation were established, as a basis for analyzing the degree of recrystallization and concurrent precipitation, where a 25% drop in hardness from the deformed condition to the full recrystallized condition was defined as the start of recrystallization and a 2.5% increase in the electrical conductivity was defined as the start of precipitation. The recrystallized grain size was measured by the linear intercept method along both rolling and normal directions in the RD-ND cross section by polarized light optical microscopy.

#### 3 Results and discussion

# 3.1 Initial microstructure before rolling

The manganese levels in solid solution, Mnss, after

different homogenization treatments were estimated based on thermoelctrical power (TEP) measurements, and the results are listed in Table 2. The Mn content in solid solution in the alloy is changed by two homogenization treatments, where the C2-1 sample has a higher value than the C2-2 sample.

The morphology and distribution of constituent particles and dispersoids after the two different homogenization treatments are illustrated in Fig. 1. The microstructure of the C2-1 material after homogenization at a higher temperature (600 °C) is shown in Fig. 1(a). Most of the eutectic networks are broken up, and constituent particles become coarsened and spheroidized. For the C2-2 material which was homogenized at a lower temperature (450 °C), there is nearly no change for the constituent particles in comparison with the as-cast state. The eutectic constituent particles still keep the rod-like or plate-like shapes. Most of the constituent particles have been measured by SEM-EDS to be Al<sub>6</sub>(Mn, Fe) and only a small fraction of constituent particles are of the  $\alpha$ -Al(Mn, Fe)Si type. This structure is similar to the solidification structure of the alloy in as-cast state which is in accordance with the earlier work [12,13]. From the quantitative analysis listed in Table 3, it is clear that much coarser and more spherical constituent particles are obtained in the C2-1 as compared with C2-2, which is due to the significant coarsening and growth of the particles during homogenization at 600 °C in the former case [13]. The fact that the area fraction of constituent particles in C2-1 sample is larger than that in C2-2

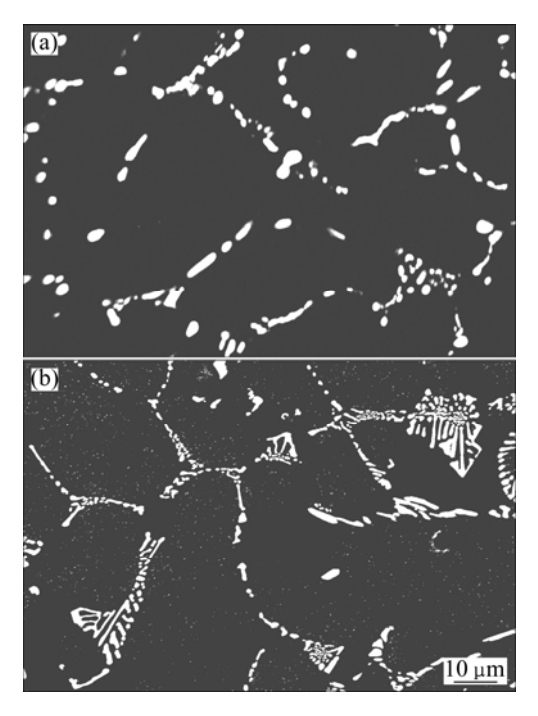


**Fig. 1** Back scatter electron SEM images of constituent particles after different homogenization procedures: (a) C2-1; (b) C2-2

**Table 3** Area fraction, mean diameter and thickness of constituent particles in four states after homogenization

	Sample	Area fraction/%	Mean diameter/μm	Feret (min)/Feret (max)	
	C2-1	2.9	1.5	0.50	
	C2-2	1.9	1.0	0.37	

sample (2.9% vs 1.9%) is mainly due to the coarsening between the fine dispersoids and large constituent particles, during heating and holding at higher temperatures (>530 °C), which makes the constituent particles grow. Furthermore, the decomposition of the supersaturated solid solution during holding at 600 °C also causes the growth of constituent particles. During the heating and holding at 450 °C, the decomposition of the supersaturated solid solution is mainly through the precipitation of dispersoids and there is nearly no change for the constituent particles due to the low diffusion rate of Mn in Al matrix [13,14].

Another difference between C2-1 and C2-2 is a lot of dispersoids distributing in grains in the latter material while such dispersoids cannot be detected in the former. In order to show more clearly the morphology and distribution of fine dispersoids precipitated during homogenization of C2-2, high magnification electron backscattered images were taken, as shown in Fig. 2. The chemical compositions of the dispersoids measured by SEM-EDS show that the dispersoids are of  $\alpha$ -Al(Mn, Fe)Si type. For the C2-1, the dispersoids precipitated during heating have dissolved during holding at 600 °C for 24 h. This is caused by the mechanism that nucleation of dispersoids in 3xxx alloys mainly occurs in the low temperature range (300-450 °C) during heating, while at higher temperatures the evolution of dispersoids is mainly controlled by coarsening and dissolution [14]. The size parameters of the dispersoids in C2-2, including Feret diameters ((min) and (max)), were quantitatively measured and the size distribution of the dispersoids is shown in Fig. 3. C2-2 contains a large percentage of small dispersoids with Feret (min) lower than 200 nm.

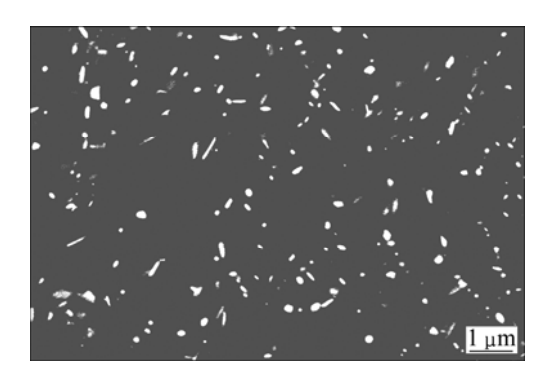


**Fig. 2** Back scatter electron SEM image of precipitated particles in C2-2 after homogenization

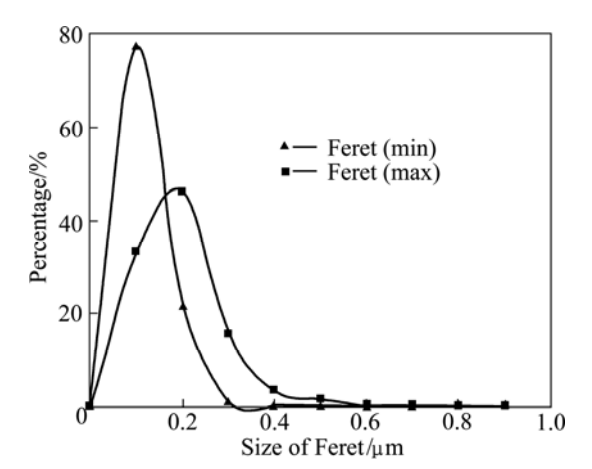


**Fig. 3** Size distribution of precipitated particles after homogenization in C2-2

#### 3.2 Softening behavior

The softening behaviours of the C2-1, in view of Vickers hardness (VHN), electrical conductivity (EC) and TTT-diagram, are shown in Fig. 4, where the behaviours at three different temperatures are compared, i.e. 350, 400 and 500 °C, marked with solid-dash lines in

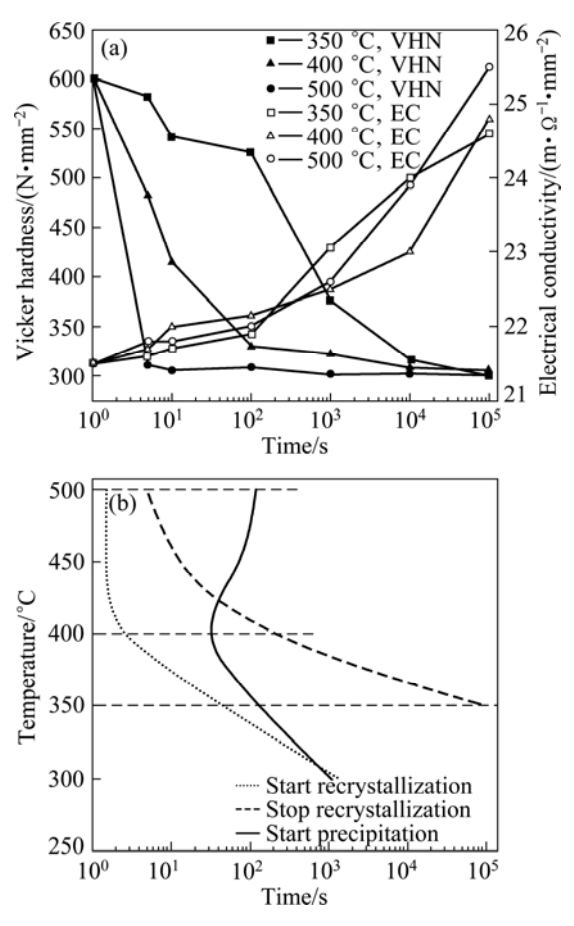


**Fig. 4** Vickers hardness and electrical conductivity for C2-1 with true strain of 1.6 during isothermal back-annealing at 350 °C, 400 °C and 500 °C for different time (a) and TTT-diagram for C2-1 with true strain of 1.6 (b)

Fig. 4(b). After the C2-1 with a true strain of 1.6 was annealed at 350 °C, it took close to 10<sup>5</sup> s to finish the softening process, and during this period a large number of dispersoids precipitated from the matrix, as indicated by the increase of electrical conductivity in Fig. 4(a) (especially at time >100 s). The concurrent precipitation has a strong influence on the softening behavior (Fig. 4(a)), resulting in a coarse grain structure (average grain size along RD and ND: 40 and 20 µm, respectively, Fig. 5(a)). During annealing at 400 °C, recrystallization finished within only a few hundreds of seconds, and during this period only a small number of dispersoids did precipitate from the matrix (Fig. 4(a)). In this case concurrent precipitation has a very limited influence on the softening behavior (Fig. 4(b)), resulting in a fairly fine grained structure (average grain size along RD and

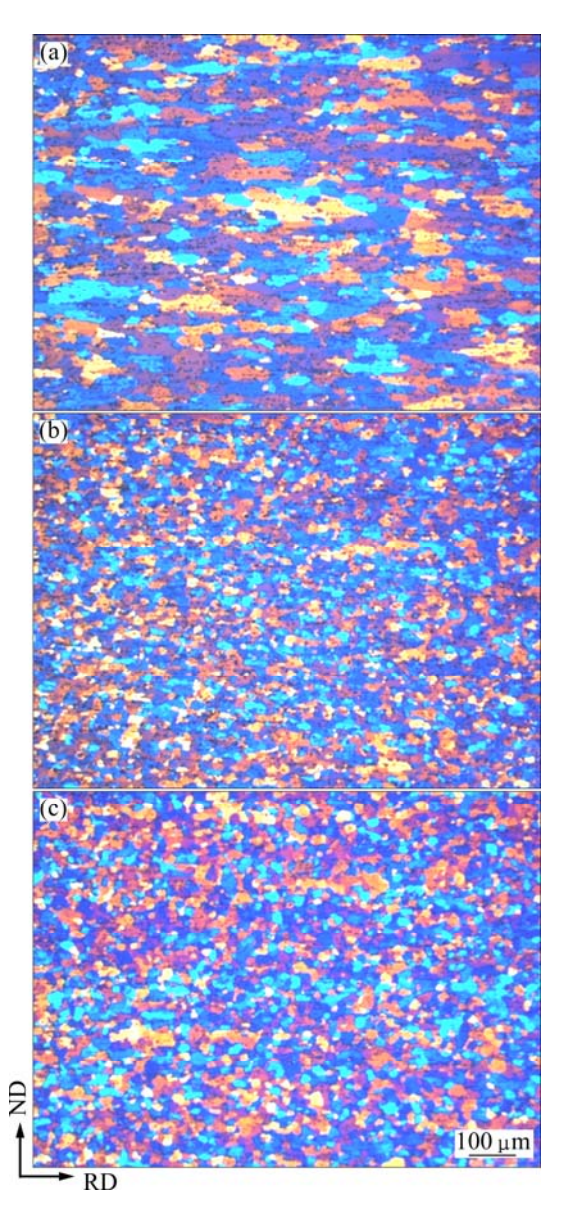


**Fig. 5** Recrystallized grain structure in C2-1 with true strain of 1.6 after isothermal back-annealing: (a) At 350 °C for 105 s; (b) At 400 °C for 105 s; (c) At 500 °C for 105 s

ND: 19 and 16  $\mu$ m respectively, Fig. 5(b)). With the highest annealing temperature of 500 °C, recrystallization finished well before precipitation started (Fig. 4(b)), namely, recrystallization occurred without any influence of precipitation. As a result, a homogeneous fine grained structure was also obtained in this case (average grain size along RD and ND: 21 and 16  $\mu$ m respectively, Fig. 5(c)).

The annealing behaviours of the C2-2 as-rolled to a strain of  $\varepsilon$  =1.6, in view of the evolution in Vickers hardness (VHN) and electrical conductivity (EC) during back-annealing and TTT-diagram, are shown in Figs. 6(a) and (b), respectively. Three different annealing temperatures, 400, 450 and 500 °C, marked with solid-dash lines in Fig. 6(b), are compared. After being annealed at 400 °C for 10<sup>5</sup> s, the softening process was not completed yet. The softening process is even slower than in C2-1. This is because a large number of fine dispersoids pre-existing in the alloy before backannealing (formed during homogenization, see Fig. 2) give rise to a strong retarding force, a Zener drag, which hinders the recrystallization. As a result, inhomogeneous and coarse grain structure is obtained, as shown in Fig. 7(a). When the C2-2 was annealed

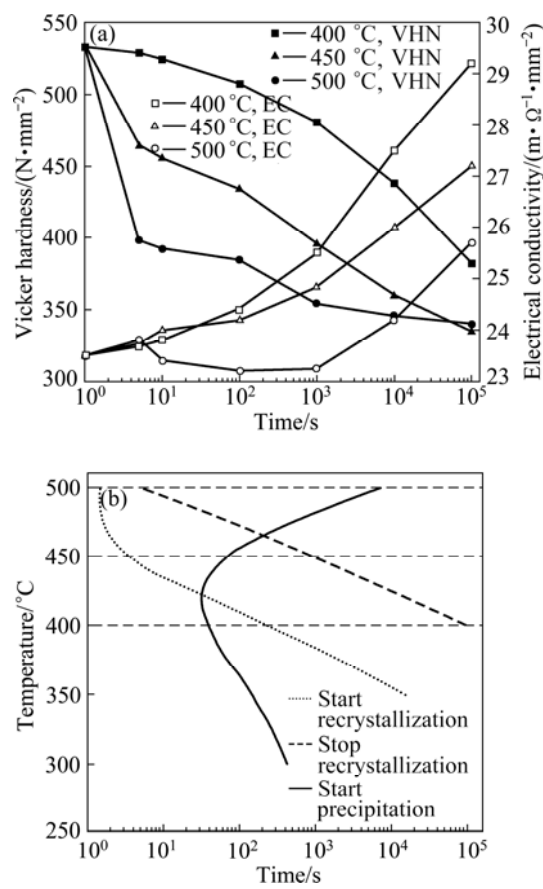


**Fig. 6** Vickers hardness and electrical conductivity of C2-2 with true strain of 1.6 during isothermal back-annealing at 400, 450 and 500 °C for different time (a), TTT-diagram for C2-2 with true strain of 1.6 (b)

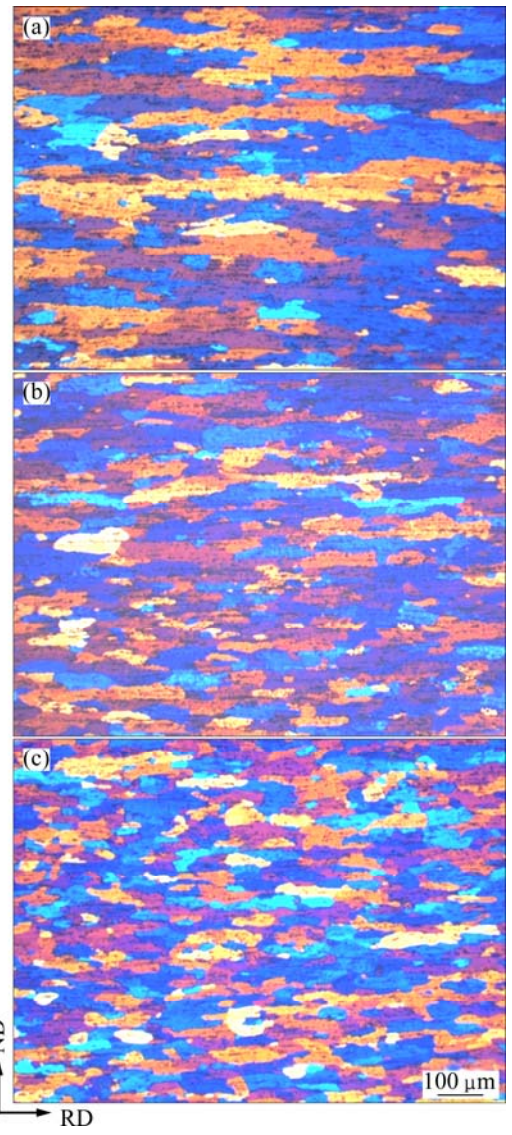


**Fig. 7** Recrystallized grain structure in C2-2 with true strain of 1.6 after isothermal back-annealing: (a) At 400 °C for 10<sup>5</sup> s; (b) At 450 °C for 10<sup>5</sup> s; (c) At 500 °C for 10<sup>5</sup> s

at 450 and 500 °C, although softening finished in a shorter time, the grain size of the material is also much coarser than the C2-1 after the same annealing treatments. This means that even during back annealing at high temperatures, the pre-existing fine dispersoids have a significant retarding effect on the recrystallization.

The Zener drag can be expressed through the formula  $P_Z = \alpha \gamma_{\rm gb} f/r$ , where f is the volume fraction, r is the mean size of dispersoids, and  $\gamma_{\rm gb}$  is the grain boundary energy [1]. As expressed by this formula, a high volume fraction, f, of fine dispersoids (small r) promotes a large Zener drag, exactly what we have in the C2-2, where the pre-existing dispersoids in the as-homogenized condition are present with a high density/volume fraction (also consistent with the low Mn<sub>ss</sub> level in this condition) with a mean diameter of 100 nm, explaining the strong influences observed.

The examples discussed above are in line with general knowledge that second-phase particles in general have a strong effect on the softening behavior. Large constituent particles typically with a size larger than 1 µm, are surrounded by a large amount of dislocations after deformation. Thus the driving pressure for activation of recrystallization is locally increased and gives rise to the phenomenon of particle stimulated nucleation (PSN) of recrystallization. On the other hand, a large number of small closely spaced particles (dispersoids) will retard the migration of both low and high angle grain boundaries (Zener pinning) and tend to hinder/retard recrystallization. As a consequence, the recrystallization behavior and resulting grain structure depend on the evolution and precipitation of dispersoids during back-annealing. Recrystallization controlled by the former effect, with recrystallization grains originating from a large number of randomly distributed PSN nucleation and/or grain boundary (GB) sites, generally result in a homogeneous fine grained structure. When the latter effect (a large number of small dispersoids) dominates the recrystallization process, the density of nucleation sites (potential sites pinned by dispersoids) for recrystallization is decreased. In addition to suppress nucleation, a pronounced Zener drag will slow down the recrystallization reaction itself. Moreover, as the dispersoids tend to precipitate and line up in the RD-TD plane (boundaries/sub-boundaries of the pancake-shaped deformed grains, see Fig. 6(c)), leading to larger Zener pinning in the direction normal to the rolling plane [15], a coarse inhomogeneous grain structure with pancake shape elongating along the rolling direction will occur, consistent with the observations of the present investigation. The difference between the C2-2 and the C2-1, investigated in this work, is that in the former case a high density of pre-existing fine dispersoids (present before back annealing) gives a large static Zener drag, while in the latter case concurrent precipitation gives a dynamic Zener drag that increases during the course of the softening reaction. However, the effect on the softening behaviour is similar in the sense that the kinetics is slowed down and in both cases a coarse grained structure is obtained.

#### **4 Conclusions**

Two different homogenization procedures gave different Mn contents in solid solution and dispersoids of different size and densities. These materials were further cold rolled to different strains before back-annealing at different temperatures. It is shown that the softening behavior is strongly influenced by annealing temperature, dispersoid size and densities and amount of Mn in solid solution. Both high annealing temperature and a well

homogenization (reducing Mn levels in solid solution and therefore less potential for concurrent precipitation) promote fast recrystallisation and the formation of a homogeneous fine grained structure. Pre-existing dispersoids and concurrent precipitation both have a significant influence on the recrystallization behavior, where especially high density fine pre-existing dispersoids strongly suppress nucleation and/or retard recrystallization (through the Zener pinning pressure), resulting in a sluggish recrystallization reaction and an inhomogenous coarse grain structure.

# Acknowledgements

This research work has been supported by a KMB project (193179/I40), in Norway. The financial support by the Research Council of Norway and the industrial partners, Hydro Aluminium and Sapa Technology is gratefully acknowledged.

#### References

- HUMPHREYS F J, HATHERLY M. Recrystallization and related annealing phenomena [M]. Oxford, United Kingdom: Elsevier Science Ltd. 1995.
- [2] HUMPHREYS F J. The nucleation of recrystallization at second phase particles in deformed aluminium [J]. Acta Metallurgica, 1977, 25(11): 1323–1344.
- [3] VATNE H E, ENGLER O, NES E. Influence of particles on recrystallization textures and microstructures of aluminium alloy 3103 [J]. Materials Science and Technology, 1997, 13(2): 93-102.
- [4] DAALAND O, NES E. Recrystallization texture development in

- commercial Al-Mn-Mg alloys [J]. Acta Materiallia, 1996, 44(4): 1413-1435.
- [5] HJELEN J, ØRSUND R, NES E. On the origin of recrystallization textures in aluminium [J]. Acta Metallurgica et Materialia, 1991, 39(7): 1377-1404.
- [6] CHAN H M, HUMPHREYS F J. The recrystallization of aluminium-silicon alloys containing a bimodal particle distribution [J]. Acta Metallurgica, 1984, 32(2): 235–243.
- [7] HUMPHREYS F J, KALU P N. Dislocation-particle interactions during high temperature deformation of two-phase aluminium alloys [J]. Acta Metallurgica, 1987, 35(12): 2815–2829.
- [8] NES E, EMBURY J D. Phase transformations during recrystallization in aluminium alloys [J]. Metallkd Z, 1975, 66: 589–593.
- [9] DAALAND O, DRONEN P E, VATNE H E, NÆSS S E, NES E. On the growth rate of cube-, rotated cube-, and rotated goss-grains in commercial aluminium alloys [J]. Materials Science Forum, 1993, 113–115: 115–120.
- [10] NES E. The effect of fine particle dispersion on heterogeneous recrystallization [J]. Acta Metallurgica, 1976, 24: 391–398.
- [11] KWAG Y, MORRIS J G. The effect of structure on the mechanical behavior and stretch formability of constitutionally dynamic 3000 serious aluminium alloys [J]. Materials Science and Engineering, 1986, 77: 59-74.
- [12] BACKERUD L, KROL E, TAMMINEN J. Solidification characteristics of aluminium alloys: Wrought alloys, vol. 1 [M]. Skanaluminium, Oslo: Universitetsforlaget AS, 1986: 93–97.
- [13] LI Y J, ARNBERG L. Evolution of eutectic intermetallic particles in DC-cast AA3003 alloy during heating and homogenization [J]. Materials Science and Engineering A, 2003, 347: 130–135.
- [14] LI Y J, ARNBERG L. Quantitative study on the precipitation behavior of dispersoids in DC-cast 3003 alloy during heating and homogenization [J]. Acta Materialia, 2003, 51: 3415–3428.
- [15] NES E, RYUM N, HUNDERI O. On the Zener drag [J]. Acta Metallurgica, 1985, 33(1): 11–22.

# AlMnFeSi 合金退火过程中的微观组织及力学性能的演变

王 宁¹, Jarl Erik FLATØY¹, 李彦军², Knut MARTHINSEN¹

1. Department of Materials Science and Engineering, Norwegian University of Science and Technology, NO-7491, Trondheim, Norway;

2. SINTEF Materials and Chemistry, NO-7465, Trondheim, Norway

摘 要:通过 2 种不同的均匀化热处理及随后的冷轧,使一种 3xxx 系模型合金获得不同尺寸和分布的弥散析出相,并使铝基体含有不同含量的 Mn。系统研究不同均匀化热处理组织和冷轧变形量对退火过程中模型合金的回复与再结晶行为的影响。根据实验结果,绘制出弥散析出相和再结晶过程的相互作用时间—温度—转变曲线 (TTT)。TTT 曲线显示固溶体中 Mn 的含量和弥散析出相的颗粒密度对软化行为有强烈的影响。在再结晶退火过程中或再结晶退火之前析出的高密度、细小、弥散析出相显著阻碍软化过程,并形成粗大的再结晶组织。在没有细小、稠密的弥散相影响下的再结晶退火,可以获得均匀、细小的等轴晶。而且,弥散析出相对再结晶过程的阻碍作用取决于再结晶过程的持续时间和弥散析出相的数量。在持续时间长的再结晶过程中,细小、稠密的弥散相对再结晶有着强烈的影响,而在其他情况下影响则有限。不管再结晶过程中是否受到弥散相析出的影响,在再结晶退火之前已经存在于组织中的细小、稠密的弥散相(平均尺寸 0.1 μm)也会导致再结晶退火之后形成粗大的再结晶组织。关键词:均匀化热处理:弥散析出相;固溶体;退火,再结晶:TTT-图;同步析出